Experimental Investigation of Weld Quality for Dissimilar Welding of AA6061-T6/AA7075-T6 Aluminum Alloys

M. Safari[a,*], **R.A. de Sousa**[b], **J. Joudaki**[a], **H. Mostaan**[c]

[a]Mechanical Engineering Department, Arak University of Technology, Arak, Iran.

[b]Mechanical Engineering Department, University of Aveiro, Campus de Santiago, Aveiro, Portugal.

[c]Materials and Metallurgical Engineering Department, Arak University, Arak, Iran.

Article info

Abstract

In this article, the friction stir welding of dissimilar AA6061-T6/AA7075-T6 aluminum alloys was studied experimentally. The joining process was implemented with and without the addition of the TiO_2 nanoparticles. To infer the resulting quality, tensile tests were carried out and the microstructure of the welded samples was investigated by the optical microscope. Furthermore, the samples were welded using gas tungsten arc welding (GTAW) to provide further comparisons with the FSW process. The ultimate tensile strength and maximum elongation increased by 12.3 and 12.5% respectively by adding TiO_2 nanoparticles. Microstructure observation shows that equiaxed grains formed in the FSW process and no precipitation aging occurred in the melting zone -however, precipitation particles can be observed in the heat-affected zone. Coarser grains can be obtained by adding TiO_2 nanoparticles, resulting in good dispersion at the stir zone and retarding the dynamic recrystallization (pinning the grain boundary movements). The sample welded by the GTAW process showed very weak strength compared to the samples welded by the friction stir welding process.

1. Introduction

The welding process is a permanent joining method to connect different parts together. Due to increasing the temperature to the melting or softening temperature of the material, metallurgical and mechanical changes are produced in the welding zone and its neighbor zone. The welding method is selected according to the type of welded materials (chemical composition, similar or dissimilar joining and melting temperature of the sheets), the need for filler material, the deposition rate of the filler metal and geometrical characteristics of the weld (welding position, thickness of sheets, and depth of penetration). Among the different welding processes, Friction Stir Welding (FSW) process is a solid-state joining process, which used widely in welding of similar and dissimilar metals particularly aluminum alloys. The FSW process is considered as the most important improvement in metal joining in the former decades. The fusion welding can lead to the melting of the aluminum alloys and consequently, the strength of the joint decreases due to the formation of Al_2O_3 composition. In the FSW process, a particularly-shaped cylindrical tool rotates and penetrates into the workpiece. The plunging of the tool continues until the shoulder of the tool reaches the top surface of the workpiece and then the tool moves along the welding seam at a constant rate. The rotational movement of the tool generates heat and the regions around the FSW tool are softened due to the frictional heat. The shoulder

avoids flowing the softened material outward. Accordingly, a weld joint is made by extrusion and forging of thermally softened material from the leading side to the trailing side of the rotating tool. Consequently, the two different sides of the weld line, which are called advancing, and retreating side may have different properties. The friction stir welding process has few mechanical and metallurgical benefits compared to the fusion welding processes. The FSW process is used widely in different industries such as automobile industries. The friction stir welding of dissimilar alloys, mainly in aluminum alloys, has some restrictions. Hitherto, a number of researchers have investigated the effects of weld parameters on the strength and mechanical properties of welded dissimilar aluminum alloys. The main controllable process parameters are the material type, rotational speed, pin profile, and feed rate. The effects of process conditions investigated in the friction stir welding of dissimilar aluminum alloys [1-4]. The joint strength depends on the quality of the welding procedure and the weld quality influences the material mixing during dissimilar friction stir welding. The rotational and the feed rate are the main influencing parameters on appropriate material mixing. Jamshidi Aval et al. [5] studied the FSW of dissimilar aluminum alloys (AA5086-O and AA6061-T6). The material mixing improved at higher rotational speed and lower feed rate. The profile of the pin can create the desirable mixing flow in the weld zone, which determines the joint strength and leads to the absence of defects [5, 6]. Moreover, further studies revealed that a bulky volume of the material was just extruded around the retreating side and then deposited behind the pin, i.e. lack of complete stirring in the welding zone [7]. The location of welding pairs (where the alloy is in the advancing or in the retreating side) can vary the mechanical strength and the quality of materials bonding of dissimilar alloys in the friction stir welding. The alloy location pointedly can improve the material flow [1] or affect the chemical composition of the nugget [2] and the formation of intermetallic particles. Additionally, the thermal distribution has a noteworthy effect on mechanical properties and weld quality [8]. Mishra and Ma [9] comprehensively discussed different aspects of FSW and friction stir processing(FSP) in a review article in 2005. Furthermore, in a similar article published lately in 2017 by Ma et al. [10], the significant advances in the FSW and FSP were summarized. FSP established according to the basic principles of the FSW process.

The joint strength depends on controllable factors and uncontrollable factors. Statistical tools can be used for finding the optimum condition of welding. Among the different techniques of the design of experiments method (DOE), the Taguchi method and Response Surface Method (RSM) are more appropriate for statistical analysis of joint strength by the FSW

process. Devaiah et al. [11], Wakchaure et al. [12] and Ugrasen et al. [13] used the Taguchi method for finding the optimal condition of FSW process implementation in order of best mechanical properties. Devaiah et al. [11] studied the joining of AA5083 and AA6061 aluminum alloys. The effectiveness of each process parameter was determined by using an analysis of variance (ANOVA). The ANOVA results showed that the rotational speed, traverse speed, and tool tilt angle are the most significant factors. Additionally, a similar study was directed by Ugrasen et al. [13] to weld AA6061 and AA7075 aluminum alloys. The results showed that the contribution of rotational speed, feed rate, and the number of FSW passes on the strength of the weld is 63%, 24%, and 13% respectively. Jagathesh et al. [14] studied the influencing factors on joint strength of AA2024 and AA6061 dissimilar friction stir welding using Box–Behnken response surface methodology. Statistical analysis showed that the optimum tensile strength is obtained at 500rpm rotational speed and 40mm/min traverse speed.

Sharifi Asl et al. [15] investigated the joining of dissimilar AA6063-T4 aluminum alloy and AZ31B-O magnesium alloy sheets by using the FSW process. A special groove was designed to combine the TiO_2 nanoparticles within the stir zone. The FSW process leads to the formation of Al_3Mg_2 and $Al_{12}Mg_{17}$ intermetallic compounds and adding the nanoparticles and formation of intermetallic compounds can considerably increase the joint strength and the hardness. Madhu et al. [16] studied the fabrication of aluminum-based composites by Friction stir processing (FSP). The unannealed TiO_2 particles (about $1\mu m$ size) were dispersed into the commercially pure aluminum matrix by 6 passes of FSP and the FSP passes led to the formation of Nano-size particles in the matrix. The microstructural observation showed that Al_3Ti intermetallic compounds and Al_2O_3 ceramic compounds are created which leads to an increase in the joint strength and decrease in the ductility. Mirjavadi et al. [17] investigated the effect of adding TiO_2 nanoparticles in FSW of AA5083 alloy plates. A square pin tool was used for welding. The optimized rotational speed of 710rpm and feed rate of 14mm/min condition was obtained and then the AA5083+TiO_2 nanoparticles welded plates undergoes to multi-pass FSW process (from 1 to 4 passes). The results showed that the hardness and strength of samples were increased by 40% and 25% respectively after four passes of FSW. Also, better wear resistance and lower friction coefficients obtained for samples prepared by four passes of FSW.

AA7075 aluminum alloy is an interesting alloy which has been welded to different alloys by many types of research. Rajakumar and Balasubramanian [18] established relationships between mechanical properties of six different aluminum alloys (AA1100,

AA2219, AA2024, AA6061, AA7039, and AA7075) and optimized process parameters. Ahmed et al. [19] studied the FSW of AA7075-T6 and AA5083-H111 (for similar and dissimilar joints). The welding process was carried out by 300rpm rotational speed of and different traverse speeds (50, 100, 150, and 200mm/min). Microstructural studies showed that recrystallization and grain refinement occur in friction stir welding. Significant grain refining happened in the nugget zone of AA7075 while relatively coarser grains were obtained in AA5083 joints. The ultimate tensile strength varied between 245-267MPa and maximum elongation between 3 to 5.6%. Shahabuddin et al. [20, 21] investigated the effect of tool geometry and the environment of welding (underwater) on the strength and hardness of welded AA7075-T6 aluminum alloys. Saravanan et al. [22] investigated the properties for friction stir welded AA6061-T6 and AA7075-T6 aluminum alloys and the effect of process parameters was discussed. Subsequently, the most appropriate conditions for FSW welding were proposed. Moreover, the effect of heat input on the joint strength of AA6061-T6 and AA7075-T6 aluminum alloys calculated by Saravanan et al. [23]. The results showed that maximum strength can be obtained by welding with the intermediate heat conditions. The formation of finer grains and good material mixing in the stir zone are the leading reasons for the enhanced strength. Ramesh Babu and Anbumalar [24] used the FSW process for joining AA7075-T6 and AA6061-T6 aluminum alloys by varying the input parameter namely the rotational speed at constant feed rate and load. The tensile strength and the surface hardness of the stir zone increased with an increase in the rotational speed. Nouri and Kazemi Nasrabadi [25] studied the fracture behavior of the AA7075-T6 alloy joint made by FSW. Substantial plastic deformation occurred around the notch tip, which showed the elastic-plastic behavior of the welded joint. Ductile failure was developed according to the load-carrying capacity of the friction stir welded samples. Chetan et al. [26] investigated the friction stir welding of AA6061T6 and AA7075T651 aluminum alloy. Furthermore, TIG welding was conducted and the hardness of the welded samples was measured. The welded samples by FSW showed higher hardness in comparison to the welded samples by TIG welding. Safari and Joudaki [27] studied the friction stir welding of AA 6061-T6 and AA 7075-T6 aluminum alloys by developing a 3D coupled thermo-mechanical finite element model according to the Coupled Eulerian-Lagrangian (CEL) method. The model was used to predict the material flow as well as the defect formation during the FSW process explicitly and precisely. Additionally, a similar study was conducted by Alavi Nia and Shirazi [28].

The friction stir welding of AA7075 and AA6061 aluminum alloy is of great importance and interest, due to the wide usage of the aluminum alloys in the aeronautic industry. AA6061 alloys are high strength, high corrosion resistance, and lightweight aluminum that have high ductility and toughness. Meanwhile, AA7075 exhibit super high strength that has been used extensively in aircraft component and other highly stressed applications. Both materials of the AA6061 series and AA7075 series are extensively employed in marine fittings, automobiles, and aircraft applications. Both aluminum alloys are used for the manufacturing of structural parts, modern seats, tubes and their fittings in the aircraft. Hence, their weldability is important for different applications. Among the recent researches in the field of FSW, the researches focus on the dissimilar joining of AA7075 and AA6061 aluminum alloy, which is listed above [1, 13, 22-24]. Some researches [1, 13] used annealed alloy in their investigations, while precipitation hardening is an important mechanism of strengthening in the aluminum alloys. The annealed alloy is too soft to be used in the aerospace industry, i.e. yield strength about 100MPa. But T6 artificial gaining heat treatment can increase the yield strength to about 250MPa. In most of the researches previously published [22-24] on the FSW of AA6061-T6 and AA7075-T6 aluminum alloys, the attitude was the investigation of process parameters. As mentioned in the literature review, adding TiO_2 nanoparticles can increase the strength and hardness of the welded samples mostly because of grain refinement. Another main contribution of the current study is the determination of the role of adding TiO_2 nanoparticles in dissimilar welding of precipitation hardening aluminum alloys. In the current work, the microstructural and mechanical properties of friction stir welds between the AA7075-T6 and AA6061-T6 aluminum alloys (hardened by artificial aging) was investigated. For this purpose, dissimilar friction stir welding of AA7075-T6 and AA6061-T6 aluminum alloys was studied with and without the addition of the TiO_2 nanoparticles. The tensile test was used for assessing the joint weldability. It should be declared that the FSW of AA7075-T6 and AA6061-T6 aluminum alloys had not been studied until then.

2. Material and Methods

In this section, the joining of dissimilar sheets by friction stir welding procedure with and without adding TiO_2 nanoparticles is introduced, then welding by GTAW process is pronounced and at last, the sample preparation for tensile test and microstructure exploration are explained.

2.1. FSW Procedure

AA6061-T6 and AA 7075-T6 aluminum alloys are two common alloys in the industry. The strengthening of both alloys was done by precipitation hardening and

artificial aging. In addition, the friction stir welding process implies a considerable hot working on the samples, the thermomechanical process leads to recrystallization and grain refinement in the FSW process. The magnitude of applied thermomechanical load (including the temperature and material flow) has an important role in the strength of joints. The dimensions of the welded sheet were 100×100×6mm (length-width-thickness). A simple fixture was prepared to clamp the sheets in their position for butt joint welding. The chemical compositions of the workpieces are reported in Table 1 and Table 2 for AA7075-T6 and AA6061-T6 aluminum alloys respectively.

The FSW tool was designed and fabricated from H13 hot work tool steel. The diameter of the shoulder was 20mm with a 20° conical threaded pin (5mm diameter at shoulder face, 4.7mm length). Fig. 1 shows the prepared tool for the FSW process. Due to the high hardness and low machinability of tool material, the initial part was heat-treated. The annealing process was carried out at 900°C (holding time 1 hour) and cooled in the furnace. After then, the machining operation was performed to prepare the desired shape of the tool. A secondary heat treatment operation was done to harden the tool. The H13 tool steel has 4-5% Chromium alloy and considerable Molybdenum, Vanadium, Silicon alloy, which shifts the Continuous Cooling Temperature (CCT) diagram to the right side and high hardness can be obtained even by applying low cooling rate. Consequently, the tool heated up to 1020°C (holding time 25 minutes) and was quenched in the oil. Tempering heat treatment was done at 530°C. The Vanadium and Chromium element can create Vanadium Carbide and Chromium Carbide compositions that lead to high-temperature corrosion and erosion resistance and improved thermal fatigue properties. Thus, the H13 steel tool is a good choice for the FSW tool. Table 3 shows the chemical compositions of H13 tool steel.

Fig. 2 shows the designed fixture to clamp the sheets in their proper position while penetration and traverse of the tool and also restricts the transverse force in the welding. A milling machine was used for welding. After some trial and error, the rotational speed of 710 revolutions per minute (rpm) and feed rate 28mm/min was selected to implement the experimental tests. The angle of the spindle (tilt angle) was 3° with respect to the vertical direction. The tool tilt angle can improve the metal flow, but in the current study, the effect of tilt angle variation was not considered. After plunging the tool in the workpieces (4.7mm plunging depth equal to the height of pin), the tool rotated without longitudinal traverse to produce the required heat for implementing friction stir welding (15 seconds). The FSW process was repeated again by the addition of TiO_2 nanoparticles. The two parts of welding sheets were positioned as the square butt-welding procedure. A narrow gap (5mm width and 0.2mm height) was created by a milling tool. The TiO_2 nanoparticles filled and were compacted in the gap. The weight of TiO_2 nanoparticles was 20g. Fig. 2b shows the workpiece with the TiO_2 nanoparticles filled the gap before FSW. The particle size of TiO_2 powder was about 120nm.

Fig. 1. The prepared H13 steel tool for welding.

Table 1
The chemical composition of AA7075-T6 aluminum alloy (weight percent).

Element	Al	Zn	Cr	Mg	Mn	Cu	Fe	Si
Percent	Base	4.83	0.26	1.8	0.01	1.29	0.4	0.27

Table 2
The chemical composition of AA6061-T6 aluminum alloy (weight percent).

Element	Al	Zn	Cr	Mg	Mn	Cu	Fe	Si
Percent	Base	0.01	0.05	0.95	0.09	0.22	0.35	0.51

Table 3
The chemical composition of H13 tool steel (weight percent).

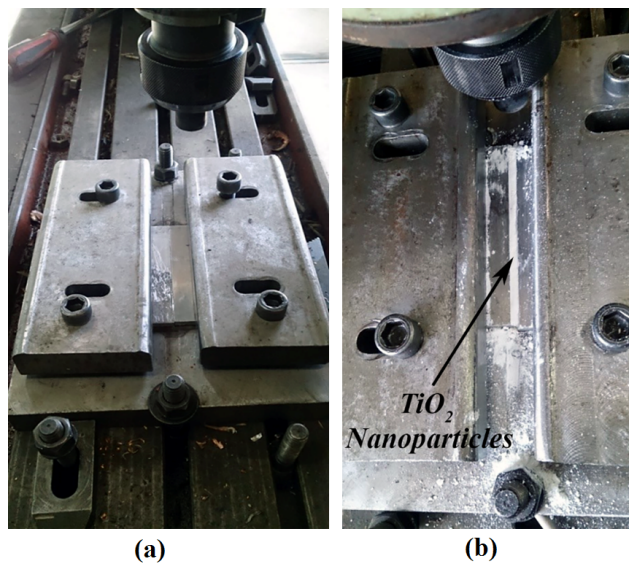| Element	Fe	Mo	V	Cr	Mn	C	Si
Percent	91.70	1.48	0.95	4.37	0.47	0.39	1.07

Fig. 2. The setup of friction stir welding a) Conventional, b) By adding TiO$_2$ nanoparticles.

2.2. GTAW Welding Procedure

Gas Tungsten Arc Welding (GTAW) or Tungsten Inert Gas (TIG) was used for joining the dissimilar aluminum alloys. The sheets were placed in the butt-welding position with a narrow gap (1mm). Alternative current (AC) was used for welding (15V and 200A). The temperature of the arc was very high (about 30,000°C) [29] and a shielding gas of Argon (25mL/min flow rate) was used to prevent the oxidation of the welded zone. The diameter of the Tungsten electrode was 3.2mm. AA4043 aluminum alloy wire (2.4mm diameter) was used as filler metal of the gap. The filler metal contains Silicon alloy which increases the penetration of molten metal in the welding zone. Silicon alloy increases the fluidity of the melt [29]. Table 4 shows the plan of experiments for different welding conditions.

2.3. Samples Preparation

After carrying out the welding, the parts were cooled in the air. A transverse cutting (perpendicular to weld seam) was done on the samples for metallographic observations. The samples were polished with sandpaper and suspension of 1μm Al$_2$O$_3$ powders. The chemical etching was implemented based on ASTM E407-2015 standard by Keller reagent (5mL HNO$_3$+ 3mL HCl+

2mL HF acid + 190mL distilled water). The holding time of samples was 14 seconds [30]. An electronic microscope was used to observe the microstructure of samples after etching. Because the aluminum metal does not have different phases, the grain boundaries can be recognized only in polarized light. Additionally, the tensile test was performed to compare the strength of the joints. The tensile test specimens were prepared according to ASTM E8/E8M-15 [31]. Fig. 3 shows the sample with its dimensions in millimeter. The test specimens were cut far enough from the initial and final part of the weld seam (at least 20mm distance) to prevent any unwanted effects in the results.
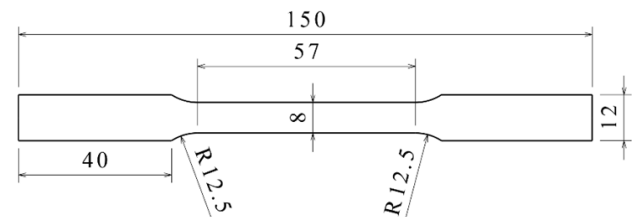

Fig. 3. a) Tensile test specimen b) Dimensions according to ASTM E8/E8M (dimensions in mm).

3. Results and Discussions

In this section, firstly, the tensile test results of welded samples are presented and finally, the results of microstructure observations are reported and discussed.

3.1. Results of Tensile Tests

Fig. 4 shows the results of tensile tests for FSW, FSW+TiO$_2$ nanoparticle and GTAW welded dissimilar aluminum welding. Fig. 5 shows the stress-strain curve obtained from the tensile test. The maximum stress of FSW samples is comparable with the strength of the base metals.

Table 4
The plan of experiments.

	Rotational speed (rpm)	Feed rate (mm/min)	Voltage (V)	Current (A)	Shielding gas Flow rate (mL/min)
FSW	710	28	-	-	-
FSW+TiO$_2$ nanoparticle	710	28	-	-	-
GTAW	-	-	15V AC	200A	25

Fig. 4. Comparison of the stress-strain curves for different welding processes.
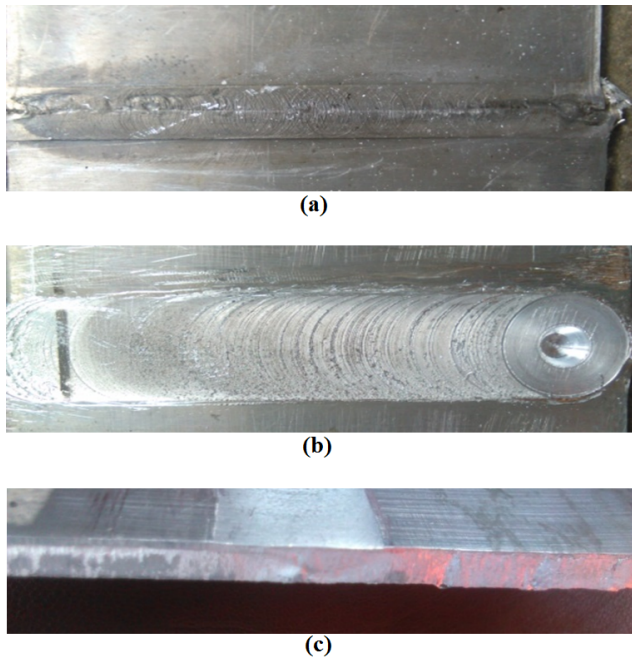

(a)

(b)

(c)

Fig. 5. The surface of friction stir welded AA7075-T6 and AA6061-T6 aluminum alloys without adding TiO$_2$ nanoparticles.

Table 5 reports the yield and ultimate tensile strength, and maximum elongation of welded specimens. The yield strength was obtained according to the standard method of proof stress (a line is drawn from 0.2% strain by the angle of the elastic modulus). The ultimate tensile stress was the maximum stress obtained in the tensile test and the maximum elongation

was determined according to the strain at failure. All of the samples failed from base metal and no fracture from the base zone was observed. FSW+TiO$_2$ nanoparticle welding showed the best joint strength for weldments. The yield strength of FSW+TiO$_2$ nanoparticle welding was almost equal to FSW (about 3% increase), but the ultimate tensile strength and maximum elongation were 12.3% and 12.5% higher than the conventional friction stir welding process, respectively. Fusion welding (GTAW) showed the worst joint strength. The yield and ultimate tensile strength reduced about 58% in comparison with FSW and FSW+ TiO$_2$ nanoparticle. The maximum elongation reduced about 64 and 68% in comparison with FSW and FSW+TiO$_2$ nanoparticle respectively. The reason for this severe decrease can be found by microstructural observation as it is discussed in the next section. The yield strength and tensile strength of AA6061T6 were equal to 276 and 310MPa. The yield strength and tensile strength of AA7075T6 were equal to 460 and 540MPa [32]. The fracture of the samples happened in the weld metal zone. It is recommended that the fracture zone of the tensile test must be out of the weld area (in the weaker base metal) for acceptable joint quality. But in real experiments, the necking happened either in the HAZ or TMAZ or weld metal. In these cases, the quality of joining was acceptable if the strength of the joining was higher than 50% of the strength of the weaker base metal [33]. The degradation effect of input heat on the filler metal and surrounding base metal leads to decreasing joint efficiency. It should be noted that the tensile test was carried out as "displacement control" and the stress-strain curve is related to the behavior of the sample under a tensile load. When the sample is loaded axially, the deformation along the longitudinal axis of the sample determines the strain. When the sample is not uniform, the total deformation depends on the deformation of base metals, TMAZ, HAZ, and welding zone. In addition, non-homogeneity affects the deformation of the sample. Thus, the stress-strain curve determines the behavior of the welded sample and different stress-strain curves can be obtained for the different conditions of the welding process. A comparison of the stress-strain curve of the FSW and FSW+TiO$_2$ nanoparticles shows that adding TiO$_2$ nanoparticles lead to enhanced strength.

Table 5
Comparison of tensile test results for samples.

	Yield strength (MPa)	Ultimate tensile Strength (MPa)	Maximum elongation (mm)	Fracture zone
FSW	234	252	5.05	Weld metal
FSW+TiO$_2$ nanoparticle	241	283	5.68	Weld metal
GTAW	100	110	1.8	Weld metal

Figs. 5 and 6 show the surface of the samples jointed by FSW and FSW+TiO$_2$ nanoparticles. The surface quality is good and no crack can be seen by the visual test (VT). Fig. 7 shows the optical micrograph of the AA7075-T6 and AA6061-T6 base metals before welding. As can be seen, both of the base metals are in the as-rolled condition and grains are aligned with the rolling direction. The black particles were seen in the base metal (BM) are strengthening precipitates but there is an appreciable difference in the size of the precipitates.
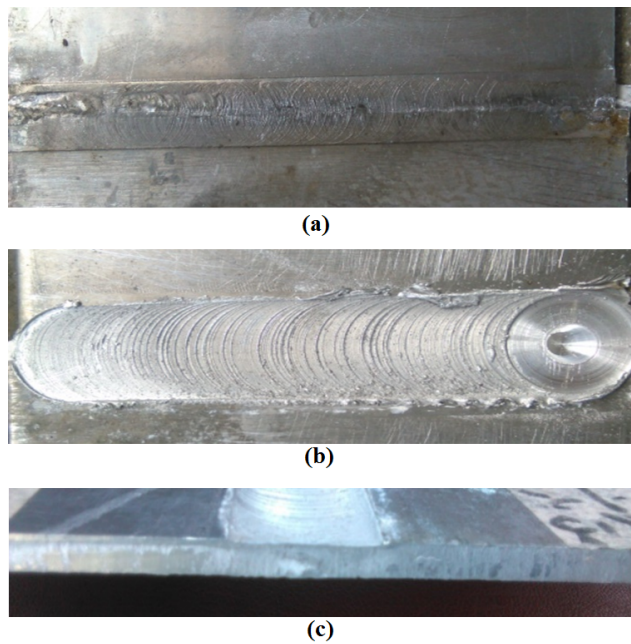

(a)

(b)

(c)

Fig. 6. The surface of friction stir welded AA7075-T6 and AA6061-T6 aluminum alloys by adding TiO$_2$ nanoparticles.

The samples were etched after welding. The AA7075-T6 aluminum alloy was at the advancing side of FSW. Figs. 8 and 9 show the microstructure of the samples jointed by FSW and FSW+TiO$_2$ nanoparticles in different zones of welding. The results show that the grains in the retreating side (AA6061-T6) recrystallized and new grains formed and grew in the heat-affected zone (HAZ). The HAZ, which is adjacent to the thermomechanical affected zone (TMAZ), experiences only a thermal cycle, without undergoing any plastic deformation. The microstructures of the heat-affected zone (HAZ) were similar for both of the alloys processed by FSW and FSW+TiO$_2$ nanoparticles welding. Moreover, it is similar to the nature of HAZs in other types of fusion welding. Although the precipitation-hardened aluminum alloys (such as AA7076 and AA 6061) are readily weldable by FSW, a severely softened region in the HAZ is expected, which is basically characterized by the dissolution or coarsening of the originally existent primary strengthening precipitates during the thermal cycle [34]. No considerable grain evolution was observed in the thermomechanical affected zone (TMAZ) and microstructure was similar to Fig. 7b. Furthermore, the results show that the grains in the thermomechanical affected zone (TMAZ) of advancing side (AA7075-T6) recrystallized and new fine grains are formed. The TMAZ experiences a lower magnitude of strains and strain rates as well as a lower peak temperature. In this region, dynamic recrystallization typically does not occur or only partially occurs. The characteristic elongated grains in the TMAZ exhibit a flow pattern around the SZ [34].

The microstructure of the FSW samples (with and without TiO$_2$ nanoparticles) are shown in Fig. 10. The figure clearly shows that the stir region consists of very fine equiaxed grains as revealed by Keller etching. The stir zone of the weld between AA7075-T6/AA6061-T6 contains fine grains without a dendritic structure. But, mixing in the stir zone does not happen in the atomic scale during FSW of dissimilar metals, and it is possible to find larger concentration differences in the base metal. Higher plastic deformation and frictional heating in the stir zone lead to dynamic recrystallization and result in fine-grained microstructure unless excessive heat is generated. It is believed that the material of the stir zone experiences severe plastic deformations at a high strain rate of 1-100s^{-1} and a cumulative strain of up to ∼40. The maximum temperatures in this region could reach 0.8-0.95 Tm, depending on the material, tool design, and operating conditions [34].
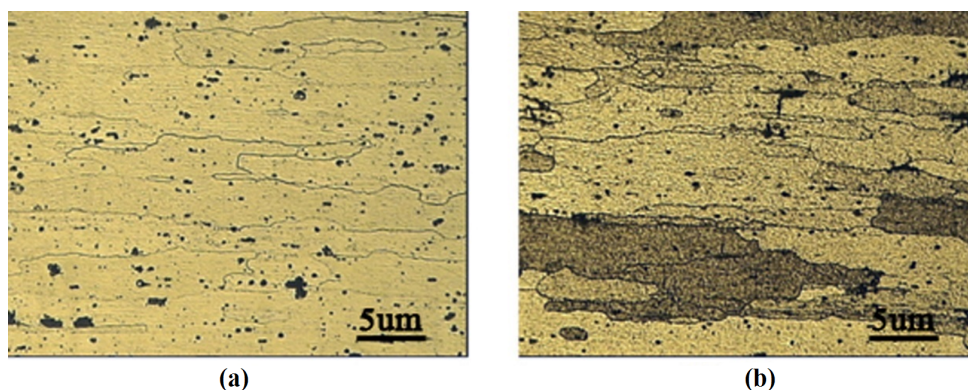

(a)   **(b)**

Fig. 7. Optical micrograph of the base metals before welding; a) AA7075-T6, b) AA6061-T6.

AA7075-T6	AA6061-T6

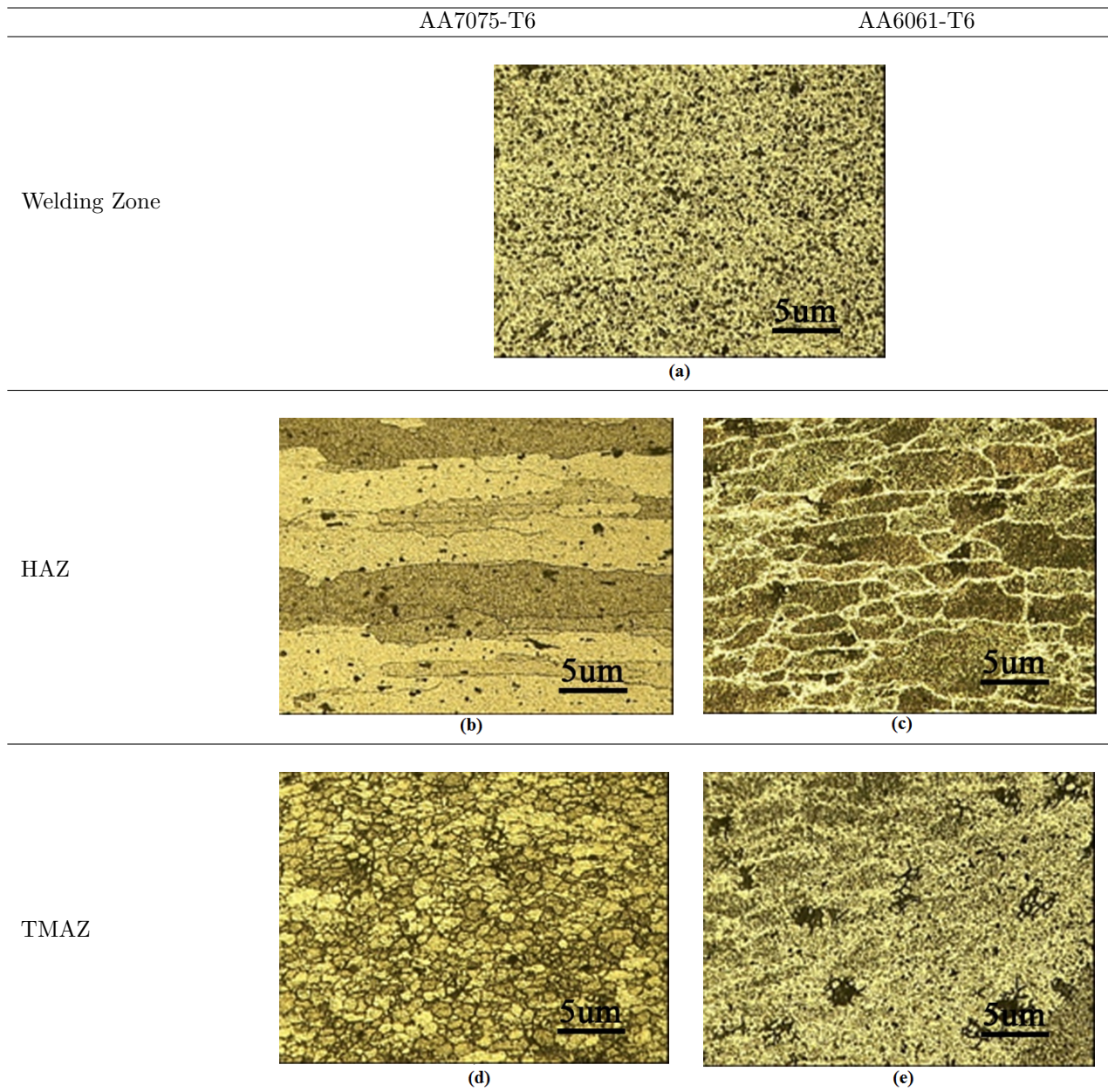
Welding Zone — (a)

HAZ — (b), (c)

TMAZ — (d), (e)

Fig. 8. Comparison of microstructure in different zones of friction stir welding.

It is worthy to note that the equiaxed grains in the stir zone of friction stir welded samples without TiO_2 particles are much finer than the FSW sample with TiO_2 particles. It appears that TiO_2 nanoparticles retard the dynamic recrystallization and restrict the grain boundary movement. Dispersion of particles exerts a retarding force or pressure on a low angle or high angle grain boundary and this may have a deep effect on the processes of recovery, recrystallization, and grain growth.

The effect is known as Zener drag. The Zener drag is defined according to two parts: (1) interaction force between a single particle and a grain boundary; and (2) the total restraining force from many particles on a grain boundary. When adding the TiO_2 nanoparticles, the second part affects the dynamic recrystallization. The second part of Zener drag is a difficult statistical problem and has not been solved yet [35].

The microstructure of the melting zone of the AA7075-T6/AA6061-T6 weld joint is shown in Fig. 11. The melting zone presents an equiaxed dendritic network. The generally fine melting zone microstructure is attributed to fast cooling rates in the associated welding.

Due to the fast cooling rate during solidification, no precipitation aging occurs in the melting zone. Precipitation aging is limited by the formation of a eutectic constituent, at the end of solidification, which takes away the most of the matrix elements needed for precipitation reactions.
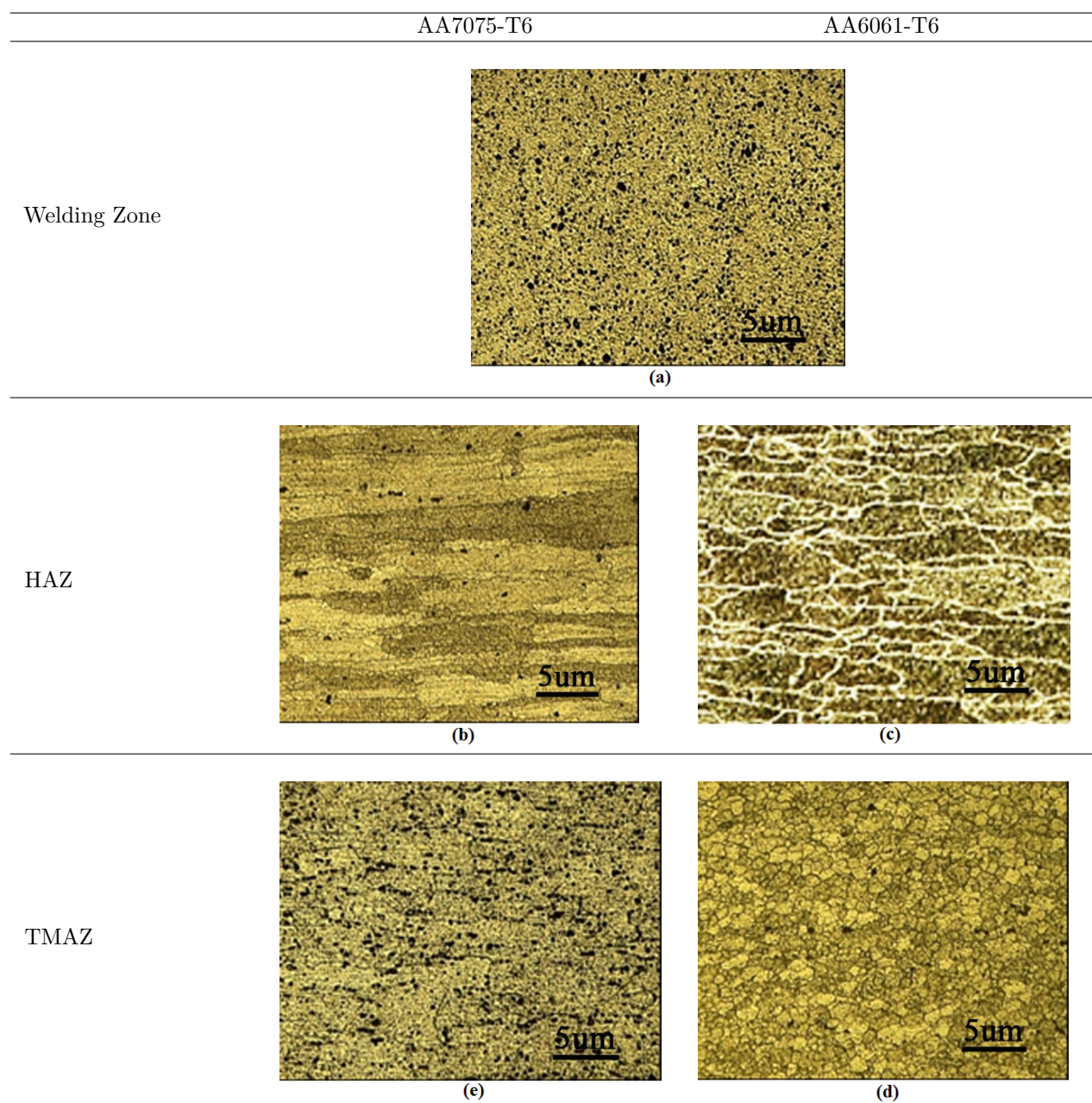
	AA7075-T6	AA6061-T6

Welding Zone

(a)

HAZ

(b)

(c)

TMAZ

(e)

(d)

Fig. 9. Comparison of microstructure in different zones of friction stir welding and adding TiO$_2$ nanoparticles.
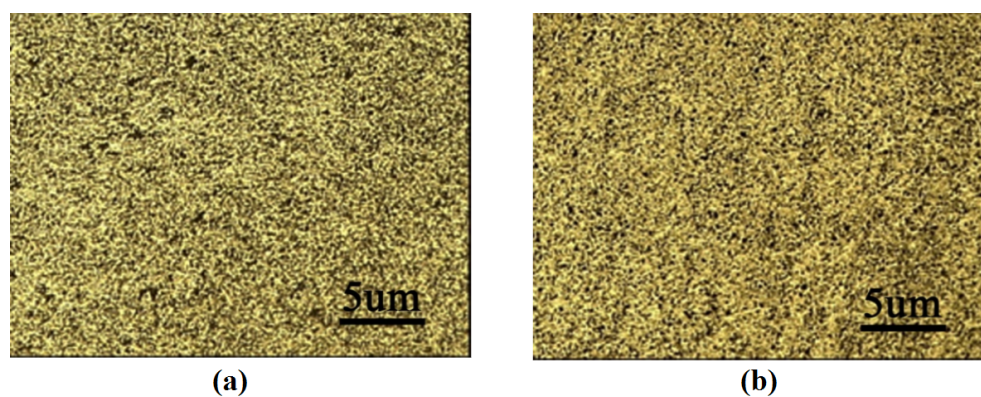

(a)

(b)

Fig. 10. Optical micrograph of welding zone in the friction stir welded samples a) Without TiO$_2$ nanoparticles, b) With TiO$_2$ nanoparticles.
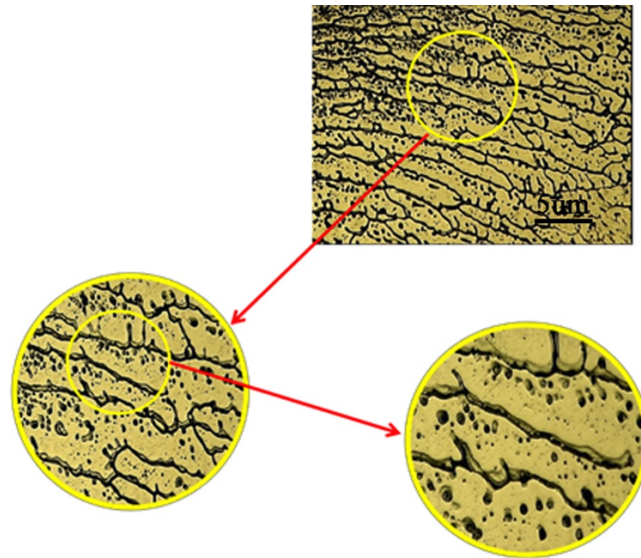
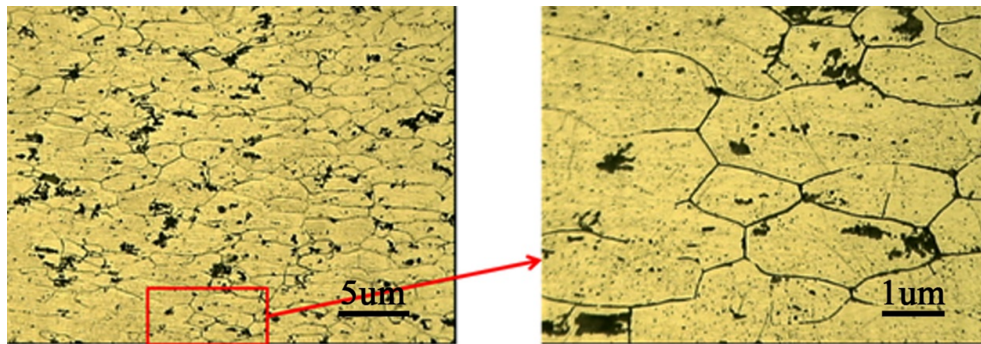**Fig. 11.** Optical micrographs of the fusion zone.

Fig. 12. Optical micrographs of the heat-affected zone.

The microstructure is mainly governed by two types of solid-state reactions in the heat-affected zone (Fig. 12): 1. dissolution or coarsening of precipitate and coarsening of grain in zone submitted to higher peak temperatures and 2. partial dissolution of precipitate and transformation of metastable phase to stable phase in the zone submitted to low peak temperature.

4. Conclusions

In this article, welding of dissimilar AA6061-T6/AA7075-T6 aluminum alloys was investigated. The main findings of this research can be highlighted as follows:

- Adding TiO_2 nanoparticles lead to a moderate increase in the tensile strength and maximum elongation (12.5%).

- The yield and ultimate tensile strength of the gas tungsten arc welded sample decreases more than 50% in comparison to the friction stir welded samples.

- The welded samples by the FSW process show suitable joint strength in comparison to the GTAW process. Adding TiO_2 nanoparticles improves the weld strength.

- Without adding TiO_2 nanoparticles, equiaxed grains are formed in the stir zone without precipitation particles. The heat-affected zone experiences the dissolution of the precipitates during the thermal cycle.

- By adding TiO_2 nanoparticles, dynamic recrystallization is retarded and no precipitation particles are formed in FSW.

- Friction stir welding (with or without adding TiO_2 nanoparticles) shows higher strength and better welding quality than gas tungsten arc welding.

- No considerable grain evolution is observed in the thermomechanical affected zone (TMAZ) in the retreating side (AA6061-T6) but in the grains in the TMAZ of the advancing side (AA7075-T6) recrystallization happens and new fine grains are formed.

- The generated heat during GTAW is very high and the aluminum alloys lose the precipitation hardening properties (T6 heat treatment). The FSW process generates moderate heat but the time of the process is considerably higher than the GTAW process. An acceptable mechanical property can be obtained by proper material mixing of the FSW process.

Compliance with Ethical Standards

Authors hereby announce that no part of this study was funded by any institutions and /or organizations. Authors also acknowledge no conflict of interests.

References

[1] J.F. Guo, H.C. Chen, C.N. Sun, G. Bi, Z. Sun, Wei, J., Friction stir welding of dissimilar materials between AA6061 and AA7075 Al alloys effects of process parameters, Mater. Des., 56 (2014) 185-192.

[2] H. Jamshidi Aval, Influences of pin profile on the mechanical and microstructural behaviors in dissimilar friction stir welded AA6082–AA7075 butt joint, Mater. Des., 67 (2015) 413-421.

[3] P. Cavaliere, A. De Santis, F. Panella, A. Squillace, Effect of welding parameters on mechanical and microstructural properties of dissimilar AA6082–AA2024 joints produced by friction stir welding, Mater. Des., 30(3) (2009) 609-616.

[4] R. Palanivel, P. Koshy Mathews, N. Murugan, I. Dinaharan, Effect of tool rotational speed and pin profile on microstructure and tensile strength of dissimilar friction stir welded AA5083-H111 and AA6351-T6 aluminum alloys, Mater. Des., 40 (2012) 7-16.

[5] H. Jamshidi Aval, S. Serajzadeh, A.H. Kokabi, Thermo-mechanical and microstructural issues in dissimilar friction stir welding of AA5086-AA6061, J. Mater. Sci., 46(10) (2011) 3258-3268.

[6] R. Palanivel, P. Koshy Mathews, I. Dinaharan, N. Murugan, Mechanical and metallurgical properties of dissimilar friction stir welded AA5083-H111 and AA6351-T6 aluminum alloys, Trans. Nonferrous Met. Soc. China, 24(1) (2014) 58-65.

[7] K.J. Colligan, Material flow behavior during friction stir welding of aluminum, Weld. J., 78 (1999) 229S-237S.

[8] P.H. Shah, V. Badheka, An experimental investigation of temperature distribution and joint properties of Al 7075 T651 friction stir welded aluminium alloys, Procedia Technol., 23 (2016) 543-550.

[9] R.S. Mishra, Z.Y. Ma, Friction stir welding and processing, Mater. Sci. Eng., R, 50(1-2) (2005) 1-78.

[10] Z.Y. Ma, A.H. Feng, D.L. Chen, J. Shen, Recent advances in friction stir welding/processing of aluminum alloys: microstructural evolution and mechanical properties, Crit. Rev. Solid State Mater. Sci., 43(4) (2018) 269-333.

[11] D. Devaiah, K. Kishore, P. Laxminarayana, Optimal FSW process parameters for dissimilar aluminium alloys (AA5083 and AA6061) using Taguchi technique, Mater. Today. Proc., 5(2) (2018) 4607-4614.

[12] K.N. Wakchaure, A.G. Thakur, V. Gadakh, A. Kumar, Multi-objective optimization of friction stir welding of aluminium alloy 6082-T6 Using hybrid Taguchi-Grey relation analysis- ANN method, Mater. Today. Proc., 5(2) (2018)7150-7159.

[13] G. Ugrasen, G. Bharath, G. Kishor Kumar, R. Sagar, P.R. Shivu, R. Keshavamurthy, Optimization of process parameters for Al6061-Al7075 alloys in friction stir welding using Taguchi's technique, Mater. Today. Proc., 5(1) (2018) 3027-3035.

[14] K. Jagathesh, M.P. Jenarthanan, P. Dinesh Babu, C. Chanakyan, Analysis of factors influencing tensile strength in dissimilar welds of AA2024 and AA6061 produced by Friction Stir Welding (FSW), Aust. J. Mech. Eng, 15(1) (2017) 19-26.

[15] N. Sharifi Asl, S.E. Mirsalehi, K. Dehghani, Effect of TiO_2 nanoparticles addition on microstructure and mechanical properties of dissimilar friction stir welded AA6063-T4 aluminum alloy and AZ31B-O magnesium alloy, J. Manuf. Proc., 38 (2019) 338-354.

[16] H.C. Madhu, P. Ajay Kumar, C.S. Perugu, S.V. Kailas, Microstructure and mechanical properties of friction stir process derived Al-TiO_2 nanocomposite, J. Mater. Eng. Perform., 27 (2018) 1318-1326.

[17] S.S. Mirjavadi, M. Alipour, S. Emamian, S. Kord, A.M.S. Hamouda, P.G. Koppad, R. Keshavamurthy, Influence of TiO_2 nanoparticles incorporation to friction stir welded 5083 aluminum alloy on the microstructure, mechanical properties and wear resistance, J. Alloys Compd., 712 (2017) 795-803.

[18] S. Rajakumar, V. Balasubramanian, Establishing relationships between mechanical properties of aluminium alloys and optimised friction stir welding process parameters, Mater. Des., 40 (2012) 17-35.

[19] M.M.Z. Ahmed, S. Ataya, M.M. El-Sayed Seleman, H.R. Ammar, E. Ahmed, Friction stir welding of similar and dissimilar AA7075 and AA5083, J. Mater. Process. Technol., 242 (2017) 77-91.

[20] Shahabuddin, V.K. Dwivedi, A. Sharma, Experimental investigation of the mechanical properties and microstructure of AA 7075-T6 during underwater friction stir welding process, Int. J. Mech. Eng. Adv. Technol., 8(4) (2019) 1289-1294.

[21] Shahabuddin, V.K. Dwivedi, Effect of tool geometry of friction stir welding on mechanical properties of AA-7075 aluminum alloy, Int. J. Mech. Eng. Technol., 9(6) (2018) 625-633.

[22] V. Saravanan, S. Rajakumar, A. Muruganandam, Effect of friction stir welding process parameters on microstructure and mechanical properties of dissimilar AA6061-T6 and AA7075-T6 aluminum alloy joints, Metallography, Microstructure, and Analysis, 5(6) (2016) 476-485.

[23] V. Saravanan, N. Banerjee, R. Amuthakkannan, S. Rajakumar, Effect of heat input on tensile properties of friction stir welded AA6061-T6 and AA7075-T6 dissimilar aluminum alloy joints, Int. J. Multidiscip. Sci. Emerging Res., 3(1) (2014) 961-965.

[24] K.R. Ramesh Babu, V. Anbumalar, An experimental analysis and process parameter optimization on AA7075 T6-AA6061 T6 alloy using friction stir welding, J. Adv. Mech. Des. Sys. Manuf., 13(2) (2019) 1-10.

[25] A. Nouri, M. Kazemi Nasrabadi, Ductile failure prediction of friction stir welded AA7075-T6 aluminum alloy weakened by a V-notch, J. Stress Anal., 4(1) (2019) 113-124.

[26] P. Chetan, P. Hemant, P. Hiralal, Experimental investigation of hardness of FSW and TIG joints of aluminium alloys of AA7075 and AA6061, Frattura ed Integrità Strutturale (Fracture and Structural Integrity), 37 (2016) 325-332.

[27] M. Safari, J. Joudaki, Coupled Eulerian-Lagrangian (CEL) modeling of material flow in dissimilar friction stir welding of aluminum alloys, Iran. J. Mater. Form., 6(2) (2019) 10-19.

[28] A. Alavi Nia, A. Shirazi, A numerical and experimental investigation into the effect of welding parameters on thermal history in friction stir welded copper sheets, J. Stress Anal., 2(1) (2017) 1-9.

[29] S. Kou, Welding Metallurgy, 2nd Ed. John Wiley and Sons Inc., New Jersey, USA (2003).

[30] https://www.metallographic.com/Metallographic-Etchants/Metallography-Aluminum-etchants.htm, 2020.

[31] ASTM E8/E8M–15a Standard Test Methods for Tension Testing of Metallic Materials, American Society for Testing and Materials: West Conshohocken (2015).

[32] https://www.Matweb.com, 2020.

[33] M. Ashby, R. Messler, R. Asthana, E. Furlani, R.E. Smallman, A.H.W. Ngan, R.J. Crawford, N. Mills, Engineering Materials and Processes Desk Reference, 1st Ed. Butterworth-Heinemann, Oxford, UK (2009).

[34] R. Nandan, T. Debroy, H.K.D.H. Bhadeshia, Recent advances in friction-stir welding–process, weldment structure and properties, Prog. Mater. Sci., 53(6) (2008) 980-1023.

[35] E. Nes, N. Ryum, O. Hunderi, On the Zener drag, Acta. Mater., 33(1) (1985) 11-22.